Title

3,3',4,4',5-Pentachlorobiphenyl (PCB 126) Decreases Hepatic and Systemic Ratios of Epoxide to Diol Metabolites of Unsaturated Fatty Acids in Male Rats.

Journal

Toxicological Sciences, 152(2)

ISSN

1096-6080

Authors

Wu, Xianai

Yang, Jun

Morisseau, Christophe

et al.

Publication Date

2016-08-01

DOI

10.1093/toxsci/kfw084

Peer reviewed

OXFORD

SOT | Society of Toxicology
www.toxsci.oxfordjournals.org

TOXICOLOGICAL SCIENCES, 152(2), 2016, 309–322

doi: 10.1093/toxsci/kfw084
Advance Access Publication Date: May 13, 2016
Research Article

3,3′,4,4′,5-Pentachlorobiphenyl (PCB 126) Decreases Hepatic and Systemic Ratios of Epoxide to Diol Metabolites of Unsaturated Fatty Acids in Male Rats

Xianai Wu,* Jun Yang,† Christophe Morisseau,† Larry W. Robertson,* Bruce Hammock,† and Hans-Joachim Lehmler*,[1]

*Department of Occupational and Environmental Health, College of Public Health, The University of Iowa, Iowa City, Iowa and †Department of Entomology and Nematology, UC Davis Comprehensive Cancer Center, University of California, Davis, California

[1]To whom correspondence should be addressed at The University of Iowa, Department of Occupational and Environmental Health, University of Iowa Research Park, no. 221 IREH, Iowa City, IA 52242-5000. Fax: (319) 335-4290. E-mail: hans-joachim-lehmler@uiowa.edu.

ABSTRACT

Disruption of the homeostasis of oxygenated regulatory lipid mediators (oxylipins), potential markers of exposure to aryl hydrocarbon receptor (AhR) agonists, such as 3,3′,4,4′,5-pentachlorobiphenyl (PCB 126), is associated with a range of diseases, including nonalcoholic fatty liver disease and nonalcoholic steatohepatitis. Here we test the hypothesis that PCB 126 exposure alters the levels of oxylipins in rats. Male Sprague-Dawley rats (5-weeks old) were treated over a 3-month period every 2 weeks with intraperitoneal injections of PCB 126 in corn oil (cumulative doses of 0, 19.8, 97.8, and 390 μg/kg b.w.; 6 injections total). PCB 126 treatment caused a reduction in growth rates at the highest dose investigated, a dose-dependent decrease in thymus weights, and a dose-dependent increase in liver weights. Liver PCB 126 levels increased in a dose-dependent manner, while levels in plasma were below or close to the detection limit. The ratios of several epoxides to diol metabolites formed *via* the cytochrome P450 (P450) monooxygenase/soluble epoxide hydrolase (sEH) pathway from polyunsaturated fatty acids displayed a dose-dependent decrease in the liver and plasma, whereas levels of oxylipins formed by other metabolic pathways were generally not altered by PCB 126 treatment. The effects of PCB 126 on epoxide-to-diol ratios were associated with an increased CYP1A activity in liver microsomes and an increased sEH activity in liver cytosol and peroxisomes. These results suggest that oxylipins are potential biomarkers of exposure to PCB 126 and that the P450/sEH pathway is a therapeutic target for PCB 126-mediated hepatotoxicity that warrants further attention.

Key words: persistent organic pollutants; polychlorinated biphenyls; oxylipin; CYP1A; soluble epoxide hydrolase.

Oxylipins are oxygenated metabolites of polyunsaturated fatty acids (PUFAs) and regulate important biological processes, including cell proliferation, apoptosis, tissue repair, and inflammation (Li *et al.*, 2011; Newman *et al.*, 2005). Altered levels of these regulatory lipids or modulation of enzymes involved in oxylipin metabolism have been linked, eg, to organ damage (Morisseau and Hammock, 2013), development of fibrosis (Harris *et al.*, 2015), and nonalcoholic fatty liver disease and nonalcoholic steatohepatitis (Liu *et al.*, 2012; Puri *et al.*, 2009; Zein *et al.*, 2012). Changes in cytochrome P450 (P450)-dependent PUFA metabolism are a potential source of side effects for drugs that induce P450 enzymes, including CYP1As (Diani-Moore *et al.*, 2006). Several major metabolic pathways result in the formation of complex mixtures of oxylipins from PUFAs (Figure 1) (Konkel and Schunck, 2011; Li *et al.*, 2011; Rifkind, 2006): (1) Oxidation of PUFAs by P450 monooxygenases yields highly stable PUFA epoxides as well as mono-hydroxylated fatty acids (Rifkind, 2006). The PUFA epoxides are further metabolized by soluble epoxide

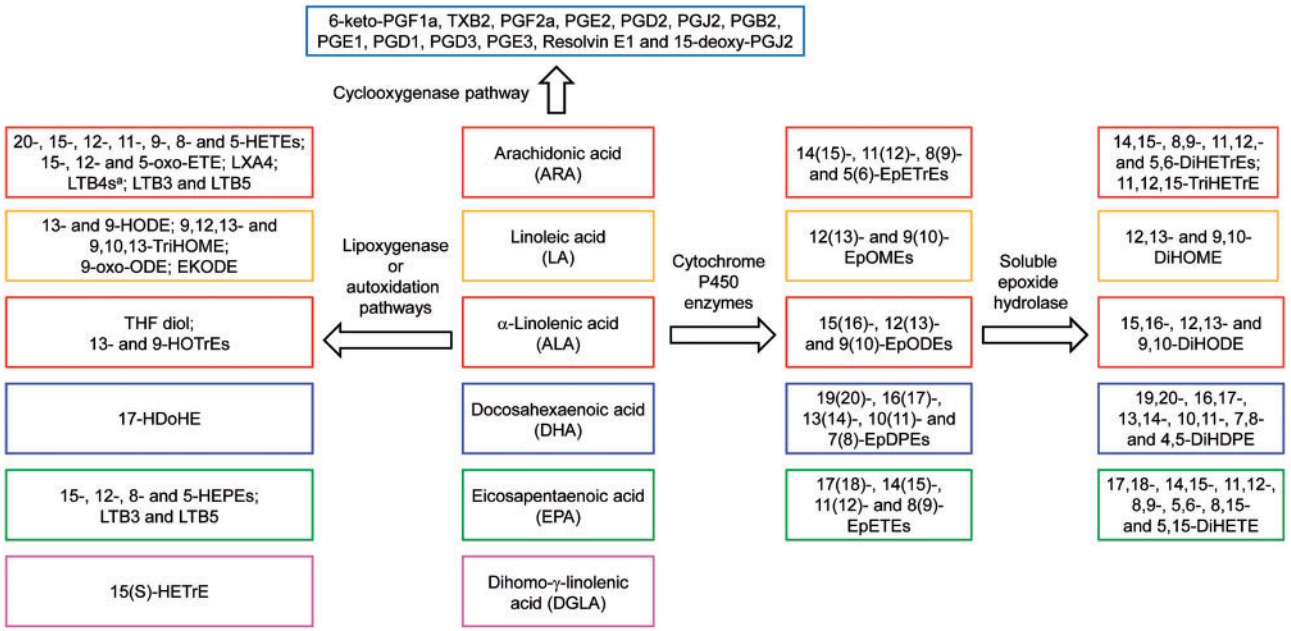

FIG. 1. PUFAs are metabolized by P450 enzymes with epoxygenase activity/sEH (P450/sEH), LOX, COX, or nonenzymatic autoxidation pathways to a number of oxylipins. Only oxylipins analyzed in this study are shown (see Supplementary Tables S6–S9 for a complete summary). [a]LTB4s include LTB4, 6-trans-LTB4, 20-OH-LTB4 and 20-COOH-LTB4. Abbreviations: DiHDPE, dihydroxy-docosapentaenoic acid; DiHETE, dihydroxy-eicosatetraenoic acid; DiHOME, dihydroxy-octadecenoic acid; DiHODE, dihydroxy-octadecadienoic acid; DiHETrE, dihydroxy-eicosatrienoic acid; EKODE, epoxy-keto-octadecenoic acid; EpDPE, epoxy-docosapentaenoic acid; EpETE, epoxy-eicosatetraenoic acid; EpETrE, epoxy-eicosatrienoic acid; EpODE, epoxy-octadecadienoic acid; EpOME, epoxy-octadecenoic acid; HDoHE, hydroxyl-DHA; HEPE, hydroxy-eicosapentaenoic acid; HETE, hydroxyl-eicosatetraenoic acid; 15(S)-HETrE, hydroxy-trienoic acid; 9-HODE, 9-hydroxy-10,12-octadecadienoic acid; HOTrE, hydroxy-octadecatrienoic acid; 6-keto-PGF1a, 6-keto-prostaglandin F1a; LTB, leukotriene B; LXA4, lipoxin A4; oxo-ETE, oxo-eicosatetraenoic acid; PGE, prostaglandin E; THF-diol, tetrahydrofurandiol; TXB, thromboxane B.

hydrolase (sEH) in the cytosol or peroxisomes to the corresponding diols (Newman *et al.*, 2005; Rifkind, 2006), with microsomal epoxide hydrolase playing a minor role (Morisseau and Hammock, 2013). (2) The lipoxygenase (LOX) pathways form hydroperoxide precursors of mono-hydroxylated fatty acids, leukotrienes and hepoxylins. (3) The cyclooxygenase (COX) pathway produces highly potent lipid mediators, such as prostaglandins, thromboxanes and prostacyclins. (4) Nonenzymatic autoxidation of PUFAs produces mono-hydroxylated fatty acids and other oxidation products. Chronic exposure to environmental contaminants can modulate the activity of key enzymes involved in the formation of oxylipins and, thus, may represent an environmental factor influencing the risk for developing these diseases by affecting oxylipins levels in target tissues, such as the liver.

PCBs are a class of environmental contaminants banned under the Stockholm Convention on Persistent Organic Pollutants. They were manufactured as complex chemical mixtures containing over 150 individual PCB congeners with different degrees of chlorination and used as cooling and insulator fluids in industrial transformers and capacitors, caulking, fluorescent light ballasts, and oil based paint (USEPA, 2013). Although their large scale industrial production was banned in the 1970s, recent studies report that PCBs are still inadvertently formed by industrial processes and are present in certain paints pigments and other chemicals (Hu and Hornbuckle, 2010). Because they are persistent in the environment and can be transported across great distances, PCBs are still detected in environmental samples and in human tissues. Human exposure to PCBs occurs primarily *via* the diet (Schecter *et al.*, 2010); however, recent animal studies suggest that inhalation of indoor and outdoor air also represents an important route of PCB exposure (Dhakal *et al.*, 2014; Hu *et al.*, 2013). Exposure to PCBs has been linked to a range of adverse health effects, including developmental neurotoxicity, carcinogenesis, and endocrine disruptive effects (Decastro *et al.*, 2006; Lauby-Secretan *et al.*, 2013; Pessah *et al.*, 2010). Growing evidence also suggests PCBs as an etiologic factor in nonalcoholic fatty liver disease (Wahlang *et al.*, 2014).

3,3′,4,4′,5-Pentachlorobiphenyl (PCB 126) is an environmentally relevant, highly toxic PCB congener of regulatory concern that causes wasting syndrome, thymic involution, inflammation, liver hypertrophy, and steatosis (Klaren *et al.*, 2016; Lai et al., 2010; NTP, 2006; Vezina *et al.*, 2004; Wang *et al.*, 2016). An evaluation of PCB 126 in a 2-year bioassay in female rats not only showed dose-dependent hepatotoxicity, but also an increase in the incidence of certain cancers, such as cholangiocarcinoma and hepatocellular adenoma (NTP, 2006). Together with other dioxin-like PCBs, it has been classified as carcinogenic to humans by the International Agency for Research on Cancer (Lauby-Secretan *et al.*, 2013). In addition, PCB 126 perturbs metal homeostasis, antioxidant levels and antioxidant enzyme activities in the liver of Sprague Dawley rats (Klaren *et al.*, 2016; Lai et al., 2010; Schramm *et al.*, 1985; Wang *et al.*, 2016). Although PCB 126 does not appear to directly alter the hepatic expression of various enzymes involved in the synthesis of oxylipins, such as COX, LOX, and sEH (Vezina *et al.*, 2004), it avidly binds to the aryl hydrocarbon receptor (AhR) (Bandiera *et al.*, 1982) and induces CYP1A1/2 enzymes *in vivo* (Lai et al., 2010; Parkinson *et al.*, 1983). Increased activity of CYP1A enzymes is a biomarker of human exposure to PCBs, polychlorinated dibenzodioxins and polychlorinated dibenzofurans (Lambert *et al.*, 2006). Similarly, TCDD (2,3,7,8-tetrachlorodibenzo-*p*-dioxin), the most potent AhR agonist, increases the expression of CYP1A1/2 in primary hepatocytes by mechanisms involving AhR activation (Rifkind,

2006). CYP1A enzymes metabolize PUFAs to various oxylipins (Konkel and Schunck, 2011; Rifkind, 2006), and altered CYP1A activity is therefore expected to affect the profile of oxylipins in the liver and the systemic circulation.

Here we test the hypothesis that chronic PCB 126 treatment alters the activity of enzymes involved in the metabolism of PUFAs, such as CYP1A enzymes, and that these changes result in concomitant effects on oxylipins levels in the male rat. To test this hypothesis, we quantified hepatic and systemic levels of 86 oxylipins derived from arachidonic acid (ARA), dihomo-γ-linolenic acid (DGLA), docosahexaenoic acid (DHA), eicosapentaenoic acid (EPA), and linoleic acid (LA) (Figure 1). Our results demonstrate that the PCB 126-mediated increase in CYP1A activity was accompanied by a significant, dose-dependent decrease in the ratios of PUFA epoxides to PUFA diols (epoxide-to-diol ratios) formed *via* the P450/sEH pathway in the liver and blood. Additional studies are therefore warranted to determine if epoxide-to-diol ratios are sensitive biomarkers of PCB 126 exposure and if the P450/sEH pathway can be targeted to attenuate hepatotoxicity caused by exposure to PCB 126 and other AhR agonists.

MATERIALS AND METHODS

Chemicals. All oxylipin standards were purchased from Cayman Chemical (Ann Arbor, Michigan). PCB 126 was synthesized by the Suzuki-coupling method from 3,4,5-trichlorobromobenzene and 3,4-dichlorophenyl boronic acid and, as describe previously, was 99.8% pure according to GC-MS analysis (Lai et al., 2010). Analytical PCB standards were purchased from AccuStandard (New Haven, Connecticut). All other chemicals were obtained from Sigma-Aldrich Chemical Company (St. Louis, Missouri) or Fisher Scientific (Pittsburgh, Pennsylvania) unless otherwise stated. 'Caution: PCBs and their metabolites should be handled as hazardous compounds in accordance with NIH guidelines.'

Animal and experimental design. The animal experiment was reviewed and approved by the Institutional Animal Care and Use Committee of the University of Iowa, Iowa City. The overall experimental design, including the rat strain, sex and route of PCB 126 administration, were selected based on several earlier studies investigating PCB 126 hepatotoxicity (Lai et al., 2010, 2011, 2012, 2013). Thirty-four male Sprague-Dawley rats (4-weeks old) were obtained from Harlan Sprague Dawley (Indianapolis, Indiana). Animals were housed in a controlled environment maintained at 22 °C with 12-h light and dark cycles. Rats were fed a basal diet (Harlan 7913 with 18% protein, 6% fat, and 5% fiber; Harlan Laboratories, Madison, Wisconsin) and water *ad libitum*. Animals were acclimatized to the animal facility for 1 week, randomized into 4 groups ($n = 8$–10 per group; average bodyweight = 147 ± 8 g) and treated every 2 weeks with intraperitoneal (i.p.) injections of corn oil (vehicle; 5 ml/kg b.w.) or PCB 126 in corn oil (5 ml/kg b.w.) for 3 months (6 injections total) with the PCB 126 doses shown in Table 1. Based on published studies (Alvarez-Lloret *et al.*, 2009; Lai et al., 2010), these doses and the dosing schedule were expected to perturb lipid and oxylipin profiles in our animal model without causing overt toxicity. Two-week after the last dose, the rats were euthanized by CO_2 asphyxiation followed by thoracotomy as confirmation of death. Blood was collected by cardiac puncture and immediately placed on ice. After the preparation of plasma, triphenylphosphine (TPP) and butylated hydroxytoluene (BHT) (10 μl of 0.2 mg/ml each in methanol) were added to a 250 μl aliquot of plasma for oxylipin analysis as described previously in Yang *et al.* (2009, 2012). All plasma samples were subsequently stored at −80 °C until oxylipin or PCB analysis. Tissues were excised *en bloc*, a piece of liver tissue (approximately 100 mg) was stabilized with the methanolic solution of TPP and BHT described earlier and stored overnight at −80 °C in 2 ml microcentrifuge tubes. Samples were shipped on dry ice to the University of California, Davis and processed upon arrival for oxylipin analysis as described below (Yang *et al.*, 2009, 2012). The remaining tissue samples were wrapped in aluminum foil, placed in liquid N_2, and transferred to a −80 °C freezer until further analysis.

PCB 126 tissue extraction procedure and analysis. PCB 126 was extracted by pressurized liquid extraction from liver and plasma samples using a Dionex ASE200 system (Dionex, Sunnyvale, California) following a published method with modifications (Kania-Korwel *et al.*, 2007). Briefly, the liver (0.40–0.63 g) and plasma (0.44–1.89 g) samples were allowed to thaw, homogeneously mixed with 2 g of diatomaceous earth (Dionex) and placed in an extraction cell (33 ml) containing Florisil (60–100 mesh, 10 g). Blank samples containing only diatomaceous earth and Florisil were analyzed in parallel. The recovery standard (2,3,4,4′,5,6-hexachlorobiphenyl, PCB 166, 250 ng; AccuStandard) was spiked to each sample and the cells were extracted with hexane/acetone (1:1, v/v) at 120 °C and 1500 psi (10 MPa) with pre-heat equilibration for 6 min, 60% of cell flush volume, and 1 static cycle of 5 min. The hexanes-acetone extracts were concentrated to approximately 1 ml using a Turbo Vap II (Biotage, LLC; Charlotte, North Carolina) and further purified as described previously (Kania-Korwel *et al.*, 2007). The PCB 126 analysis was performed on a DB1-MS (60 m × 0.25 mm ID × 0.25 μm film thickness; Agilent, Santa Clara, California) or an equity-1 capillary column (60 m × 0.25 mm ID × 0.25 μm film thickness; Supelco, Bellefonte, Pennsylvania) using an Agilent 7890A gas chromatograph equipped with 2 ^{63}Ni-micro electron capture detectors (μECD) detectors. The temperature program was as follows: 50 °C for 1 min, 30 °C/min to 200 °C, and 1 °C/min to 240 °C, and then 10 °C/min to 280 °C. The injector and detector temperatures were 280 and 300 °C, respectively. The flow rate for the carrier gas was 3 ml/min. PCB 126 levels were calculated using 2,2′,3,4,4′,5,6,6′-octachlorobiphenyl (PCB 204, 100 ng; AccuStandard) as internal standard.

The ^{63}Ni-μECDs used for the PCB 126 analysis were linear up to concentrations of 1000 ng/ml ($R^2 > 0.999$). The limit of detection (LOD) was 2.8 and 3.8 ng of PCB 126 for blood and liver, respectively, as calculated from blank samples according to the equation $LOD = \bar{x}_b + k \cdot s_b$, where $\bar{x}_b$ is the mean of 5 blank measures, k is Student's t-value for $n - 1$ degrees of freedom at 99% confidence level, and s_b is SD of the blank measures (Kania-Korwel *et al.*, 2007). The recovery of the surrogate recovery standard PCB 166 was 77 ± 8% (range: 61–101%). PCB 126 levels were adjusted for recoveries if the recovery was <100% for the individual sample.

Preparation of subcellular fractions and enzyme activity assays. Subcellular liver fractions were prepared by differential centrifugation from frozen tissue samples as described previously in Wu *et al.* (2011). In short, liver aliquots (3–5 g) were thawed on the ice and placed in ice-cold Tris-KCl buffer (pH = 7.5) with 1 mM phenylmethanesulfonylfluoride, 1 mM ethylenediaminetetraacetic acid, and 1 mM dithiothreitol. Liver homogenates were prepared from individual livers using an ULTRA TURRAX T23 basic homogenizer (IKA Laboratory Technology, Wilmington, North Carolina) and centrifuged at 9000 g for 20 min. The pellet containing the peroxisomes was resuspended

TABLE 1. Summary of Individual and Cumulative PCB 126 Dose, Expressed on a Molar, Weight or TCDD TEQ Basis, for Different Treatment Groups[a]

Group	Number of Rats	PCB 126 Dose/Injection		TCDD TEQ[b] Dose/Injection		Cumulative PCB126 Dose		Cumulative TCDD TEQ[b] Dose	
		μmol/kg b.w.	μg/kg b.w.	nmol/kg b.w.	μg/kg b.w.	μmol/kg b.w.	μg/kg b.w.	nmol/kg b.w.	μg/kg b.w.
Vehicle (corn oil)	10	0	0	0	0	0	0	0	0
Low dose	8	0.01	3.3	1	0.33	0.06	19.8	6	1.98
Medium dose	8	0.05	16.3	5	1.63	0.3	97.8	30	9.78
High dose	8	0.2	65	20	6.5	1.2	390	120	39

[a]Animals were acclimatized to the animal facility for 1 week, randomized into the 4 treatment groups, and treated every 2 weeks with i.p. injections of corn oil (vehicle; 5 mL/kg b.w.) or PCB 126 in corn oil (5 mL/kg b.w.) for 3 months.
[b]The PCB 126 dose, expressed as TCDD (2,3,7,8-tetrachlorodibenzo-p-dioxin) toxic equivalent quotient, was calculated using the 2005 WHO TEF of PCB 126 of 0.1 (Van den Berg et al., 2006).

in 10 ml of Tris-HCl buffer, and 1.5 ml aliquots were frozen in liquid N_2 and transferred to −80 °C freezer for epoxide hydrolase activity measurements. The supernatant was centrifuged further at 100 000 g for 60 min for separation of cytosol and microsomes. The microsomal pellets were resuspended in 0.25 M sucrose. Aliquots (1.5 ml) of cytosol and microsomes were frozen in liquid N_2 and transferred to −80 °C for storage.

Microsomal protein concentrations were measured as described by Lowry *et al.* (1951), with bovine serum albumin as standard. The total P450 content in microsomes was determined from CO difference spectra of dithionite-reduced microsomes using an extinction coefficient of 91 cm^{-1} mM^{-1} between A_{450} and A_{490} (Parkinson *et al.*, 1980). Microsomal ethoxyresorufin-*O*-deethylase (EROD) activity, a measure of CYP1A activity, was determined using ethoxyresorufin as the substrate. The resulting fluorescent resorufin product from the monooxygenase reaction was detected using a Perkin-Elmer LS 55 spectrofluorometer (Waltham, Massachusetts) at excitation and emission wavelengths of 550 and 585 nm, respectively, with resorufin as standard (Lai *et al.*, 2012). Epoxide hydrolase activity in cytosol, peroxisome, and microsomes were measured using racemic [^{3}H]-*trans*-1,3-diphenylpropene oxide as substrate as described in Morisseau and Hammock (2007). The activity was followed by measuring the quantity of radioactive diol formed in the aqueous phase using a scintillation counter (Tri-Carb 2810 TR; Perkin-Elmer, Shelton, Connecticut). Data for total P450 content and enzyme activities are expressed relative to controls because the subcellular fractions were generated from frozen tissue samples and likely lost activity during storage at −80°C (Pearce *et al.*, 1996).

Protein and lipids analysis in liver homogenate. Lipids were extracted following a procedure from the Kansas Lipidomics Research Center with some modification. Briefly, the liver samples (0.51 ± 0.08 g) were thawed on ice and homogenized in 10 ml of water using an ULTRA TURRAX T23 basic homogenizer (IKA Laboratory Technology). One aliquot of 1.6 ml homogenized liver was used for lipid extraction. Another aliquot of 1.0 ml homogenized liver was used for protein analysis. For the aliquot of liver sample for lipid extraction, 2 ml chloroform containing 0.01% BHT and 4 ml methanol were added to a 1.6 ml aliquot of homogenized liver sample. Samples were inverted for 5 min, followed by addition of 2 ml chloroform with BHT and 2 ml water. Samples were inverted for an additional 5 min and centrifuged at 3000 g for 5 min. The lower layer was removed (the samples were kept on ice as much as possible). The top layer was extracted 2 more times with 2 ml chloroform with BHT. The combined organic layers were washed with 0.5 ml 1M KCl and 0.5 ml water. The samples were evaporated under a gentle stream of nitrogen gas and vacuum dried in preweighted vials. Extracted lipid was weighted on a microbalance to determine the percentage of lipid in liver. Protein concentrations of liver homogenate were measured as described by Lowry *et al.* (1951), with bovine serum albumin as standard.

Oxylipins extraction and profiling by LC/MS/MS. Oxylipin extraction was performed using a modification of a previously published method Yang *et al.*, 2009, 2012). Briefly, the surrogate standard (10 μL of d_4-6-keto-prostaglandin F1a [6-keto-PGF1a], d_4-prostaglandin E2 [PGE2], d_4-thromboxane B2 [TXB2], d_4-leukotriene B4 [LTB4], d_{11}-14,15-dihydroxy-eicosatrienoic acid [DiHETrE], d_6-20-hydroxyl-eicosatetraenoic acid [HETE]), d_4-9-hydroxy-10,12-octadecadienoic acid [9-HODE], d_8-12-HETE, d_8-5-HETE, d_{11}-11(12)-epoxy-eicosatrienoic acid [EpETrE], d_4-9(10)-epoxy-octadecenoic acid [EpOME], and d_8-ARA; each at 100 nM) was spiked to TTP and BHT stabilized samples prior to extraction. Methanol with 0.1% of acetic acid and 0.1% of BHT (400 μl) was added to all liver samples (101.4 ± 16.9 mg), followed by homogenization using a Retsch homogenizer (Retsch Inc.; Newtown, Pennsylvania) at 30 Hz for 10 min. The supernatants were collected after centrifugation at 9300 × g for 10 min. The remaining pellets were washed with 100 μl of methanol, the combined supernatants were diluted with 2 ml of water and loaded onto precleaned solid phase extraction cartridges (Oasis HLB 3cc; Waters Corp., Milford, Massachusetts). Plasma (250 μl) was loaded directly onto SPE cartridges. The cartridges were washed by 2 column volumes 0.1% acetic acid in water-methanol (95:5, v/v). The samples were eluted with 0.5 ml methanol followed by 1.5 ml of ethyl acetate to tubes containing 6 μlof 30% glycerol in methanol. The extract was evaporated until the glycerol plug was left using a Jouan RC10.22 series Vacuum Concentrator (Thermo Fisher, Pittsburgh, Pennsylvania). The internal standard (50 μl of 200 nM 12- [[(cyclohexylamino)carbonyl]amino]-dodecanoic acid in methanol) was added and the samples were filtered before being transferred to HPLC vials.

The oxylipin analyses were performed using an Agilent 1200 SL liquid chromatography (Agilent; Palo Alto, California) with a 4000 QTrap tandem mass spectrometer (Applied Biosystems, Foster City, California) equipped with an electrospray source (Turbo V) and an Eclipse Plus C18 column (2.1 × 150 mm, 1.8 μm; Agilent). Gradient elution (detail in Supplementary Table S1) was performed with a mixture of mobile phase A (water with 0.1% glacial acetic acid) and mobile phase B (acetonitrile:methanol = 84:16, *v/v*, with 0.1% glacial acetic acid). Quality control samples were analyzed in parallel following a published method Yang *et al.* (2012).

Statistical analysis. The effect of PCB 126 treatment on various responses was studied using 1-way ANOVA analysis and GLM in the statistical analysis package SAS (version 9.3). Dunnett's multiple testing correction procedure was used to compare PCB 126 treatment with the corn oil control. The values are mean ± SD ($n = 10$ for control, $n = 8$ for PCB 126 treatment groups) if not mentioned otherwise. Treatment groups were considered statistically different at $P < .05$.

RESULTS

Effects of PCB 126 Treatment on Bodyweight, Organ Weight and Liver Tissue Composition

The animals received cumulative doses of PCB 126 ranging from 0.06 to 1.2 μmol/kg b.w., which is equivalent to 6–120 nmol TCDD/kg b.w. (Table 1). Rats in the high dose treatment group gained significantly less bodyweight compared with control animals beginning 2 weeks after the first PCB 126 treatment, whereas no significant effects on bodyweight gain were observed in the low and medium dose treatment groups (Figure 2A; Supplementary Table S2). Liver weights showed a clear dose-dependent increase, with a statistically significant increase in relative liver weights observed in the medium and high dose treatment groups (Figure 2B). Relative lung and spleen weights were significantly increased in the high dose treatment group, whereas relative thymus weights decreased significantly with increasing dose (Supplementary Table S4). Moreover, heart and kidney weights were significantly decreased in the high dose treatment group (Supplementary Table S3). Comparable effects on organ weights, in particular liver and thymus, following PCB 126 treatment have been reported by earlier studies Lai et al. (2010, 2011, 2012, 2013).

Protein levels and extractable lipid content was determined in the liver because PCB 126 treatment induces the expression of various hepatic enzymes, such as CYP1As, and causes fatty changes in this liver (Lai et al., 2010, 2011). Changes in both parameters contribute to the hepatic sequestration of PCB 126. Protein content in liver homogenate was significantly increased compared to controls in all 3 PCB 126 treatment groups (Figure 2C). The extracted lipid content of the liver was significantly higher compared with the control group for both the medium and high dose treatment groups (Figure 2D). This observation is consistent with an earlier, subacute PCB 126 exposure study (Lai *et al.*, 2012).

PCB 126 Levels in Liver and Plasma

PCB 126 levels in the liver and plasma were determined to allow a comparison with other animal studies (Supplementary Table S11). Levels of PCB 126 in the liver increased in a dose-dependent manner and ranged from approximately 0.13 μg/g wet weight in the low dose treatment group to 2.3 μg/g wet weight in the high dose treatment group (Figure 3; Supplementary Table S5). This 18-fold increase in PCB 126 tissue levels corresponds to the 20-fold increase in the PCB 126 dose between the low and high dose treatment groups. PCB 126 levels adjusted by extractable lipid weight displayed a similar trend and increased from 1.5 μg/g lipid in the low dose treatment group to 13 μg/g lipid in the high dose treatment group. The lipid adjusted PCB 126 levels were 9-times higher in the high versus low dose treatment group, which is 2-times less than the 20-fold increase in the external PCB 126 dose. Consistent with the relatively poor elimination of PCB 126 in the rat, a significant percentage of the total PCB 126 dose (34–45%) was sequestered in the liver. PCB 126 plasma levels in the high dose treatment group were 2.3 ng/g plasma wet weight, but were below the detection limit in the low and medium dose treatment groups.

Effects of PCB 126 Treatment on Hepatic Enzyme Activities

Dose-dependent effects of PCB 126-treatment on total P450 content, CYP1A activity and sEH activities were investigated in the liver because of their potential role in altering the disposition of PCB 126 and/or the metabolism of oxylipins. Total hepatic P450 content increased significantly in the low dose treatment group and remained significantly higher compared with the control group in the medium and high dose treatment groups (Figure 4A).

CYP1As not only plays a role in the hepatic retention of PCB 126 (Chen *et al.*, 2003; Diliberto *et al.*, 1999), but also metabolizes PUFAs epoxides (Konkel and Schunck, 2011). EROD activity, a marker of CYP1A activity (Nerurkar *et al.*, 1993), increased in a dose-dependent manner in all 3 treatment groups (Figure 4B). When compared with the control group, EROD activity increased 10-, 17-, and 21-fold in the low, medium, and high dose treatment groups. The increase in EROD activity was not directly proportional to the increase in the PCB 126 dose. For example, the EROD activity increased 10-fold from the low to high dose treatment groups, whereas the external PCB 126 dose increased 20-fold. This observation is not surprising because a nonmonotonic dose response curve for the induction of CYP1As in PCB 126-treated rats has been reported previously in Lai *et al.* (2012, 2013).

The sEH, present in the cytosol and peroxisomes, catalyzes the conversion of anti-inflammatory PUFA epoxides to the corresponding proinflammatory diols, and plays a role in balancing anti- and proinflammatory pathways (Morisseau and Hammock, 2013). Activity of sEH in cytosol showed a dose-dependent increase and was significantly higher in the high dose treatment group compared with control animals (Figure 4C). Peroxisomal sEH was significantly increased in male rats from the high dose treatment group compared with controls (Figure 4D). Microsomal epoxide hydrolase activity did not show a significant dose-dependent effect of PCB126 treatment in the present study (data not shown).

Effects of PCB 126 Treatment on Oxylipin Profile in the Liver

The dose-dependent effect of PCB 126 treatment on levels of 86 oxylipins was assessed in the liver by metabolic profiling using liquid chromatography-tandem mass spectrometry. Oxylipins were classified according to the pathways involved in their formation, including oxylipins formed by the P450/sEH, LOX, COX, and auto-oxidation pathways (Figure 1; Supplementary Tables S6–S9). The levels of oxylipins were further grouped based on the respective fatty acid precursors, such as ARA, DGLA, DHA, EPA, and LA (Figs. 5 and 6; Supplementary Figures S1–S3). Key observations can be summarized as follows:

1. Levels of 27 oxylipins changed in the liver due to PCB 126 treatment, with most changes observed for oxylipins formed *via* the P450/sEH pathway.
2. No consistent, dose-dependent change in the levels of PUFA epoxides in the P450/sEH pathway was observed in livers from PCB 126 treated animals; however, levels of most PUFA epoxides showed at least a slight increase in the liver (Figure 5). Notable exceptions were 14(15)-EpETrE, an ARA metabolite, and 19(20)-epoxy-docosapentaenoic acid (EpDPE), a DHA metabolite. Both epoxides displayed a clear, dose-dependent increase across all treatment groups. Levels of 3 out of 4 EPA

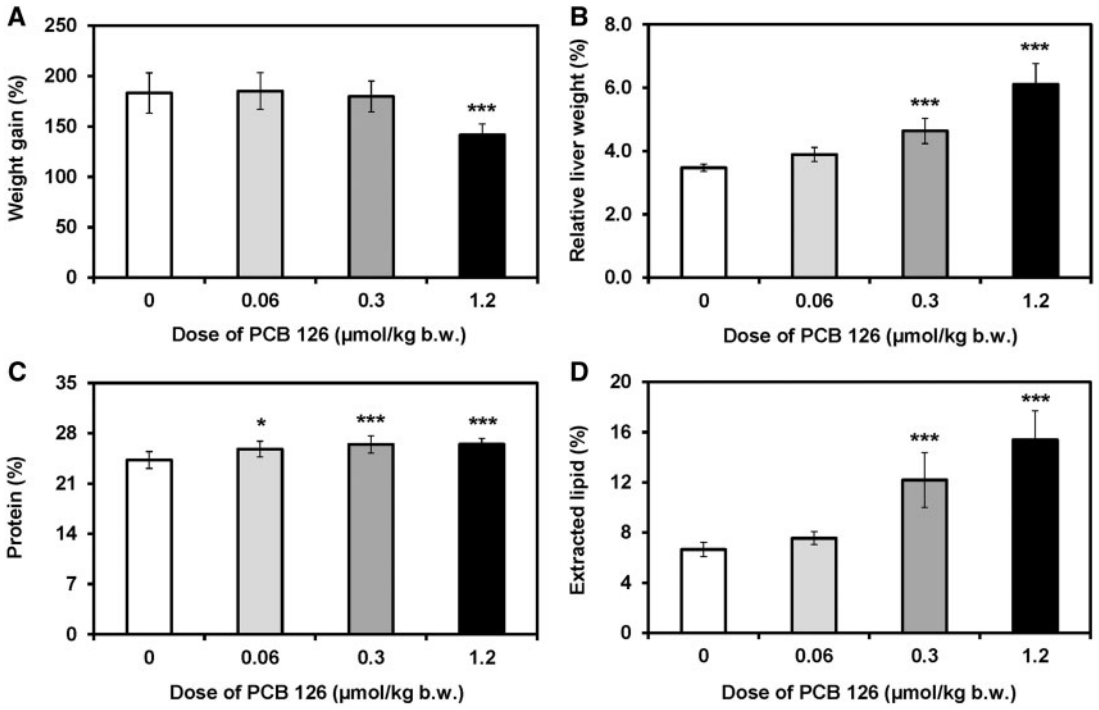

FIG. 2. Chronic PCB 126 treatment of male rats reduced **A,** body weight gain and increased **B,** relative liver weights, **C,** hepatic protein content, and **D,** extractable lipid content in liver as percent of wet weight. Rats were treated with every 2 weeks with *i.p.* injections of corn oil (vehicle) or PCB 126 in corn oil for 3 months; see Table 1 for details regarding the doses. Data are presented as the mean ± standard deviation. Dunnett's multiple testing correction procedure was used to compare PCB 126 treatment with the corn oil control. $^{*}p < .05$; $^{***}P < .001$.

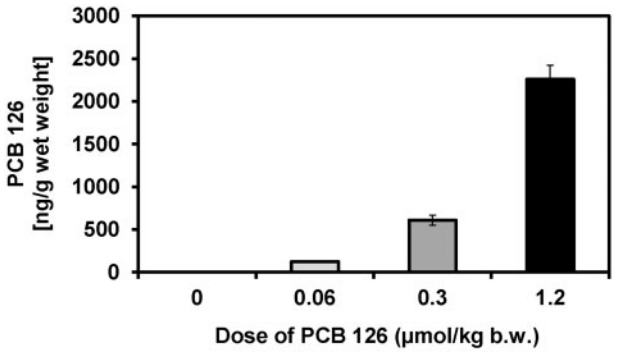

FIG. 3. PCB 126 levels in the liver increased with increasing dose. Rats were treated every 2 weeks with *i.p.* injections of corn oil (vehicle) or PCB 126 in corn oil for 3 months; see Table 1 for details regarding the doses. Data are presented as the mean ± SD.

epoxide metabolites (14(15)-epoxy-eicosatetraenoic acid (EpETE), 11(12)-EpETE and 8[9]-EpETE) were significantly increased compared with controls only in the low or medium, but not the high dose treatment groups. Similarly, levels of the ARA metabolite 5(6)-EpETrE were significantly increased in the low dose treatment group, whereas no significant difference was observed in the medium and high dose treatment groups compared with controls.

3. The following diols formed by sEH showed a statistically significant, dose-dependent increase in liver levels in the medium and high dose treatment groups (Figure 6): ARA derived oxylipins 14,15-DiHETrE, 11,12-DiHETrE, 8,9-DiHETrE, and 5,6-DiHETrE; DHA-derived oxylipins 19,20-dihydroxydocosapentaenoic acid (DiHDPE), 16,17-DiHDPE, 13,14-DiHDPE, 10,11-DiHDPE, and 7,8-DiHDPE; and EPA-derived 17,18-dihydroxy-eicosatetraenoic acid (DiHETE), 14,15-DiHETE, 11,12-DiHETE, and 8,9-DiHETE. At the same time, PCB 126 treatment had no statistically significant effect on hepatic levels of dihydroxy-octadecenoic acids (DiHOMEs) formed from LA and dihydroxy-octadecadienoic acids (DiHODEs) formed from ALA.
4. The hepatic epoxide-to-diol ratios decreased in a dose-dependent manner for several epoxides and the corresponding diols in the P450/sEH pathway (Figure 7, Supplementary Table S10). For example, these ratios significantly decreased for 5(6)-EpTrE/5,6-DiHETrE and 8(9)-EpTrE/8,9-DiHETrE, oxylipins formed from ARA, in the medium and high dose treatment groups (Figs. 7A and B, respectively). Similarly, PCB 126 treatment resulted in a dose-dependent decrease in the 16(17)-EpDPE/16,17-DiHDPE and 10(11)-EpDPE/10,11-DiHDPE (Figs. 7C and D, respectively); however, this effect was only significant in the high dose treatment group.
5. In the 12/15-LOX pathway, hepatic levels of 2 ARA metabolites, 8-HETE and lipoxin A4 (LXA4), were significantly increased in the high dose treatment group (Supplementary Figure S1). Moreover, PCB treatment significantly increased for 5-hydroxy-eicosapentaenoic acid (HEPE) and 8-HEPE, 2 EPA-derived oxylipins, in the high and medium dose treatment groups, respectively.
6. In the 5-LOX pathway, hepatic levels of LTB3 were significantly increased in all 3 treatment groups compared with controls (Supplementary Figure S2). Moreover, hepatic levels of 5-oxo-ETE, an oxylipin derived from ARA, were significantly increased in the high dose treatment group. At the same time, 20-COOH-LTB4 and 9,12,13-TriHOME significantly increased in the liver in the low and high dose treatment groups, respectively.
7. A significant, dose-dependent decrease in levels of 15-deoxy-PGJ2, an oxylipin formed *via* the COX pathway, was

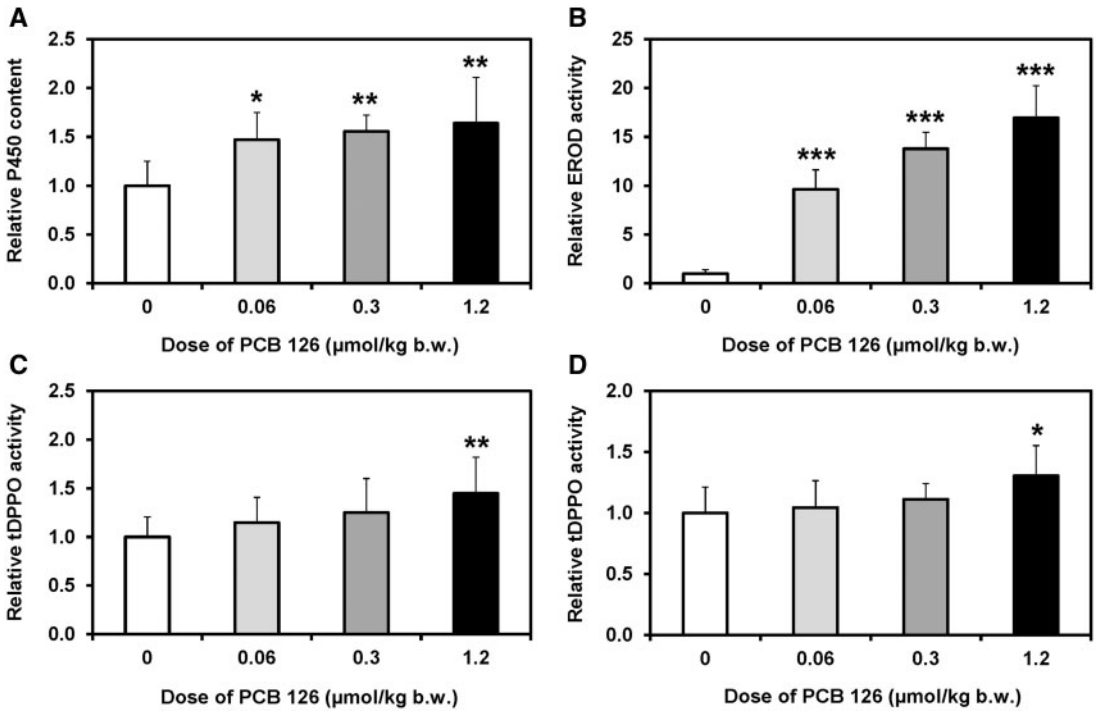

FIG. 4. Increasing PCB 126 doses resulted in an increase in **(A)** total hepatic P450 content, **(B)** EROD activity in liver microsomes as well as sEH activity in **(C)** cytosol, and **(D)** peroxisomes relative to controls. Rats were treated every 2 weeks with *i.p.* injections of corn oil (vehicle) or PCB 126 in corn oil for 3 months; see Table 1 for details regarding the doses. Data are expressed relative to controls because subcellular fractions were generated from frozen tissue samples and are presented as the mean ± SEM. Dunnett's multiple testing correction procedure was used to compare PCB 126 treatment with the corn oil control. *$P < .05$; **$P < .01$; ***$P < .001$.

observed in the liver (Supplementary Figure S3). PCB 126 treatment did not significantly alter the levels of the other 14 oxylipins in the COX pathway, which suggests that, similar to TCDD (Yang *et al.*, 2013), PCB 126 treatment did not induce COX and, possibly phospholipase A2.

Effects of PCB 126 Treatment on Oxylipin Profile in Plasma

The effect of PCB 126 treatment on levels of 86 oxylipins was also assessed in plasma and is presented based on the 4 metabolic pathways and their unsaturated fatty acid precursors (Figure 1, Supplementary Tables S6–S9). Key observations can be summarized as follows:

1. Plasma levels of 24 oxylipins changed in a dose-dependent manner in response to PCB treatment (Figs. 5 and 6, Supplementary Figures S1–S3).
2. Plasma levels of epoxy metabolites of ARA, EPA, and DHA, such as ARA-derived oxylipins 11(12)- and 5(6)-EpETrE; EPA-derived oxylipins 11(12)-EpETE; DHA-derived oxylipins 16(17)-, 13(14)-, 10(11)-, and 7(8)-EpDPE decreased in PCB 126-treated rats (**Figure 5**). The decrease in plasma levels of 16(17)-EpDPE and 13(14)-EpDPE, 2 DHA-derived oxylipins, were significantly different for controls for the medium and high dose treatment groups.
3. Plasma levels of diols metabolites of ARA, EPA and DHA formed *via* the P450/sEH pathway significantly increased with increasing PCB 126 dose (Figure 6). The most sensitive marker of PCB exposure was 5,6-DiHETrE, which was significantly increased already in the low dose treatment group. As observed in the liver, PCB 126 treatment had no effect on plasma levels of LA-derived oxylipins, such as DiHOMEs and DiHODEs.
4. The epoxide-to-diol ratios of ARA-, LA-, DHA-, and EPA-derived oxylipins in plasma decreased in a dose-dependent manner for 11 out of 18 epoxide/diol pairs investigated (Figure 8; Supplementary Table S10). For most epoxide/diol pairs, PCB 126 treatment significantly reduced the epoxide-to-diol ratios in plasma in the medium and high dose treatment groups (Figure 8). In addition, a significant difference between the low dose treatment group and controls was observed for 16(17)-EpDPE/16,17-DiHDPE and 17(18)-EpETE/17,18-DiHETE (**Figs. 8C and D**).
5. PCB 126 treatment had no significant effect on plasma levels of oxylipins formed *via* the LOX and COX metabolism pathways (Supplementary Figures S1–S3). Levels of only a few oxylipins, such as LTB4 and 6-keto-PGF1α, displayed a non-monotonic dose-response and were increased in the medium, but not the high dose treatment group.

DISCUSSION

The general toxicity of PCB 126 observed in this study includes a dose-dependent decrease of the growth rate, thymic involution, liver hypertrophy and, as suggested by the elevated hepatic lipid content, hepatic steatosis. As other studies have shown, these effects are primarily mediated by the AhR (Van den Berg *et al.*, 2006). This toxicity profile is comparable to earlier toxicity studies with PCB 126, irrespective of differences in the strain, sex, duration and route of administration among studies (Supplementary Table S11). This similarity can be explained with comparable internal PCB 126 doses (ie, hepatic PCB 126 levels) due to the hepatic accumulation of PCB 126 (Koga *et al.*, 1990; Rignall *et al.*, 2013; van Ede *et al.*, 2013). Several factors contribute to the retention of PCB 126 and other dioxin-like compounds (eg, TCDD) in the rodent liver. PCB 126 is very slowly

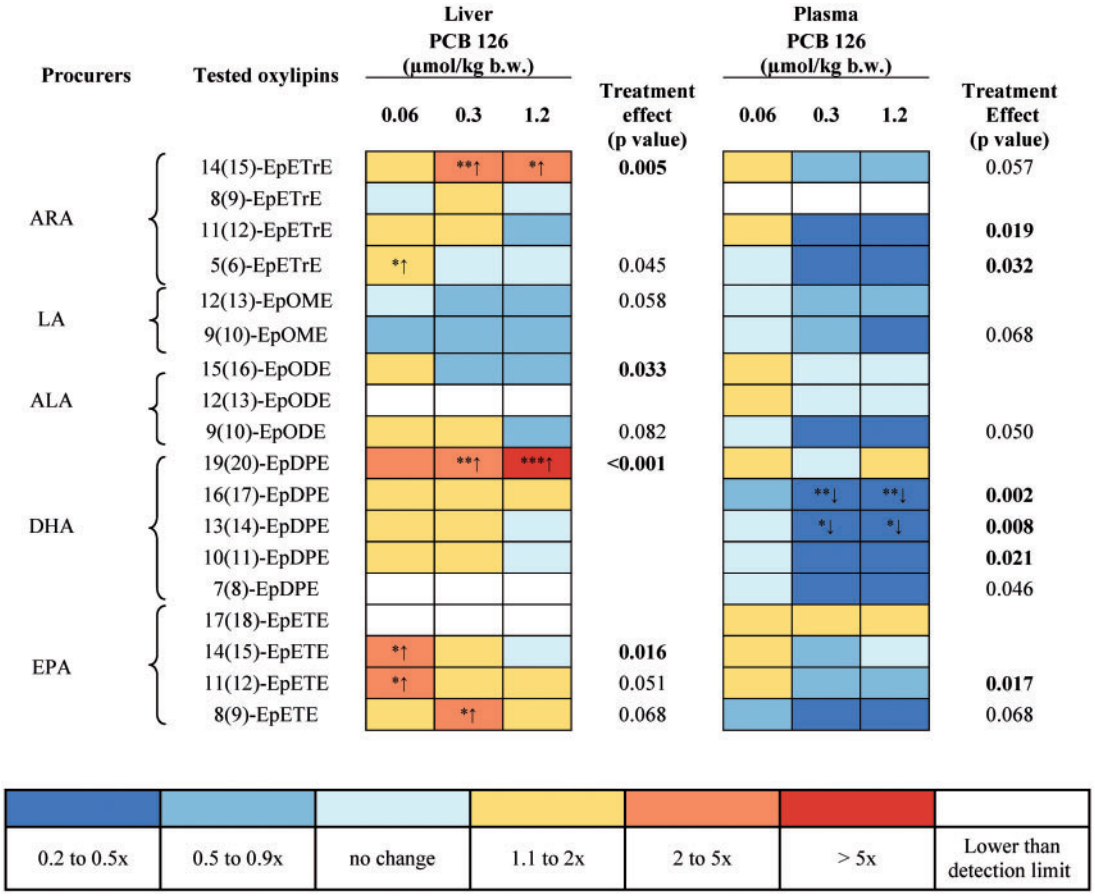

FIG. 5. 'Heat Map' presentation of the levels of epoxides in the P450 monooxygenase/sEH pathway showing some dose-dependent changes in levels of this group of oxylipins in the liver and plasma of PCB 126-treated rats. Dunnett's multiple testing correction procedure was used to compare PCB 126 treatment with the corn oil control. Significantly different from control *$P < .05$; **$P < 01$; ***$P < 0.001$. One-way ANOVA were used to test for a treatment effect.

eliminated in rodents *via* excretion from the intestinal wall and by metabolism to a hydroxylated, 1,2-shift metabolite in rats; however, PCB 126 is not readily eliminated *via* the bile (Koga *et al.*, 1990). Like other dioxin-like compounds, PCB 126 induces CYP1A2 in the liver, which results in its sequestration in the liver due to its strong binding to CYP1A2 (Chen *et al.*, 2003; Diliberto *et al.*, 1999). In addition, the increased fat content of the liver contributes to the accumulation of PCB 126 in the liver, as has been shown for other PCB congeners in models with fatty liver (Wu *et al.*, 2015). As a result, PCB 126 is distributed away from adipose tissue and other fatty tissues into the liver. Indeed, a couple of studies reported higher PCB 126 levels in the liver than in the adipose tissue of rats exposed to higher PCB 126 doses (Chu *et al.*, 1994; Van Birgelen *et al.*, 1994). Although data regarding PCB 126 levels in the human liver are limited, there is evidence that PCB 126 is likewise retained by CYP1A2 in the liver of humans (Kashimoto *et al.*, 1987; Watanabe *et al.*, 2013). PCB 126 levels in postmortem human livers range from 7 pg/g lipid to 1.5 ng/g lipid (mean = 230 ± 380 pg/g lipid) in Japanese people (Watanabe *et al.*, 2013). Similarly low levels ranging from 1.1 to 3.9 pg/g/wet weight were also reported in liver tissues from a small biomonitoring study from Belgium (Chu *et al.*, 2003). These human levels are considerably lower compared with liver levels in this laboratory study; however, the relatively high PCB 126 doses and, consequently, high tissue levels in the present study were selected based on the fundamental risk assessment principle that higher toxicant doses are needed to detect toxicity in shorter timeframes (Doull, 2003).

It is well documented that PCB 126 retained in the liver causes an AhR-mediated, dose-dependent induction of hepatic CYP1A1/2 enzymes at the mRNA, protein and activity level in rats (Fisher *et al.*, 2006; Lai et al., 2010, 2011). PCB 126 also induced the expression of both CYP1A1 and CYP1A2 at the mRNA level in primary rat hepatocytes (Xu *et al.*, 2000). In agreement with these earlier studies, hepatic EROD activity, a well-established marker CYP1A enzyme activity (Nerurkar *et al.*, 1993), increased in a dose-dependent manner in PCB 126-treated rats in our study. As demonstrated by several *in vitro* metabolism studies, rat CYP1A1 and CYP1A2 enzymes metabolize both omega-3 and omega-6 PUFAs to complex mixtures of biologically active PUFA epoxides (Konkel and Schunck, 2011). Although this has not been shown for rat P450 enzymes, studies with human P450 enzymes demonstrate that omega-3 PUFAs, such as EPA and DHA, are readily epoxidized by CYP1A2 and competitively inhibit the metabolism of omega-6 PUFAs, such as ARA (Fer *et al.*, 2008). Changes in hepatic CYP1A activities are therefore expected to alter the oxylipin profile *in vitro* and *in vivo*. Indeed, ARA is preferentially metabolized to subterminal and mid-terminal HETEs by liver microsomes obtained from rats pretreated with β-naphthoflavone or PCB 126, whereas the levels of EpETrEs and 20-HETE decrease compared with rat liver microsomes prepared from control animals (Falck *et al.*, 1990; Huang and Gibson, 1991). Similarly, LA is preferentially hydroxylated by rat liver microsomes prepared from β-naphthoflavone treated rats to HODEs (Hornsten *et al.*, 1996). A downregulation in the expression of CYP2C epoxygenases by TCDD and

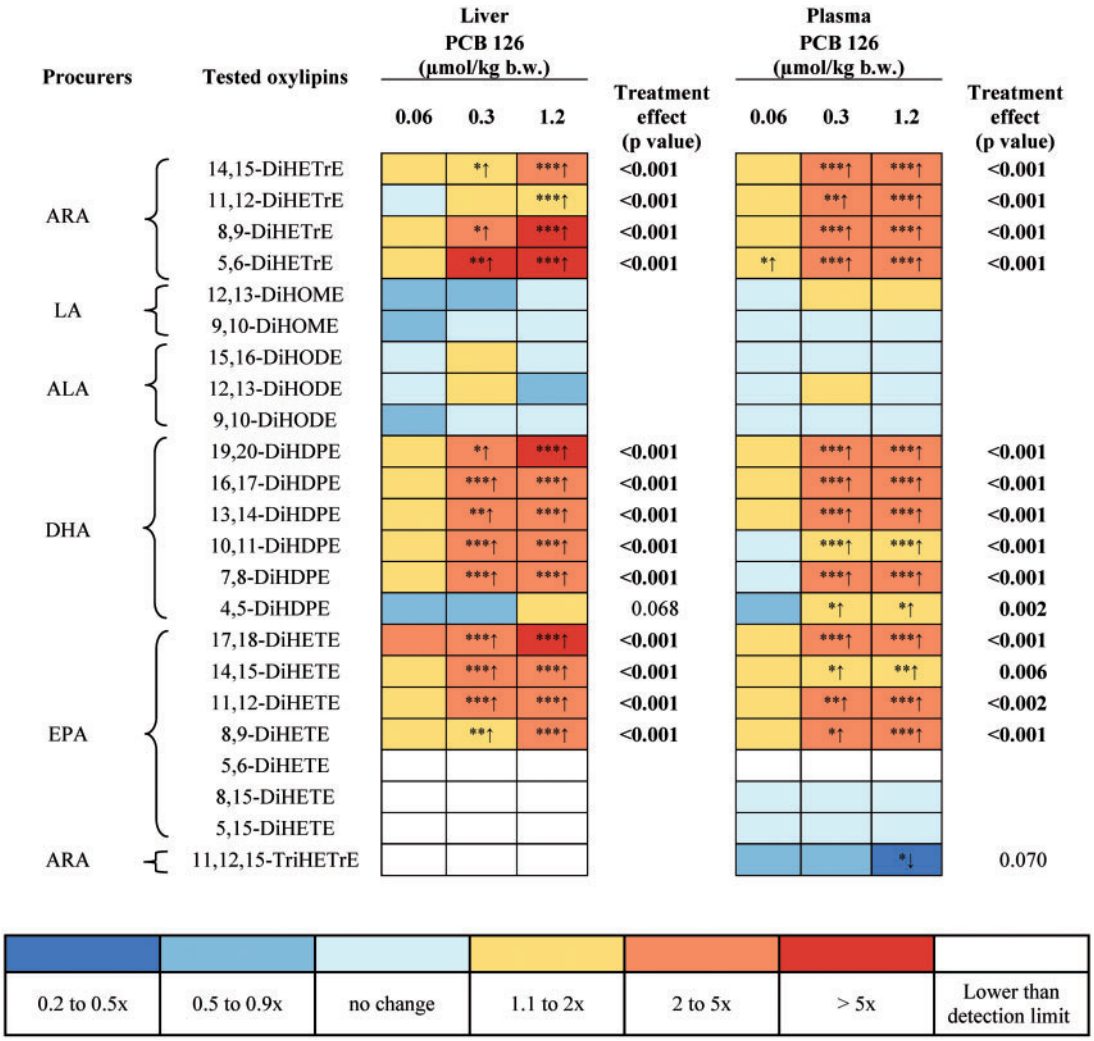

FIG. 6. 'Heat Map' presentation of the levels of diols in the P450 monooxygenase/sEH pathway showing dose-dependent changes in levels of this group of oxylipins in the liver and plasma of PCB 126-treated rats. Dunnett's multiple testing correction procedure was used to compare PCB 126 treatment with the corn oil control. Significantly different from control $^{*}P < .05$; $^{**}P < .01$; $^{***}P < .001$. One-way ANOVA were used to test for a treatment effect.

other AhR agonists (Bhathena *et al.*, 2002; Shaban *et al.*, 2005) has been suggested as an explanation for the decreased formation of PUFA epoxides in microsomal metabolism studies (Rifkind, 2006).

When compared with *in vitro* metabolism studies with liver microsomes or recombinant enzymes, changes in hepatic CYP1A activity have a more complex effect of oxylipins profiles *in vivo*. Specifically, the hepatic levels of certain PUFA epoxides increase in animal studies after induction of CYP1A enzymes following exposure to TCDD, the most potent AhR agonists (Bui *et al.*, 2012; Diani-Moore *et al.*, 2014; Yang *et al.*, 2013). This effect of TCDD on PUFA epoxide levels was not observed in AhR knockout mice (Bui *et al.*, 2012). Similarly, the present study also revealed dose-dependent effects of PCB 126-treatment on PUFA epoxide levels in the liver, in particular on levels of ARA, EPA, and DHA-derived epoxides. We noticed a pronounced, dose-dependent increase in liver levels of the ARA metabolite 14(15)-EpETrE and the DHA metabolite 19(20)-EpDPE. Levels of several other ARA, EPA, and DHA-derived epoxides were slightly increased in the liver, whereas levels of LA and α-linolenic acid (ALA)-derived epoxides seemed to decrease due to PCB 126 treatment. Similarly, a recent study of ARA metabolites demonstrated that TCDD increased the hepatic levels of 4 EpETrEs in a chick embryo model (Diani-Moore *et al.*, 2014). Moreover, acute exposure to TCDD altered the levels of several PUFA epoxides in an AhR-dependent manner in mice (Bui *et al.*, 2012; Yang *et al.*, 2013). Since CYP1A enzymes have epoxidase activity, their induction in the liver likely contributes to the increased levels of PUFA epoxides; however, the epoxidation of ARA by recombinant rat CYP1A1 and CYP1A2 displays poor regioselectivity (El-Sherbeni and El-Kadi, 2014) and, thus, may not fully explain the significant, dose-dependent increase of 14(15)-EpETrE, but not other ARA-derived epoxides. Taken together, these findings demonstrate that AhR agonists, either directly *via* AhR or indirectly by other, nonAhR-mediated mechanisms, affect multiple enzyme systems involved in the formation of PUFA epoxides. However, further studies using CYP1A1/2 knockout mice are warranted to demonstrate unambiguously that modulation of CYP1A enzyme activities alters PUFA epoxide levels *in vivo* following PCB 126 treatment.

PUFA epoxides formed by P450 enzymes are readily converted by sEH to the corresponding pro-inflammatory diols (Morisseau and Hammock, 2013). Although microsomal epoxide

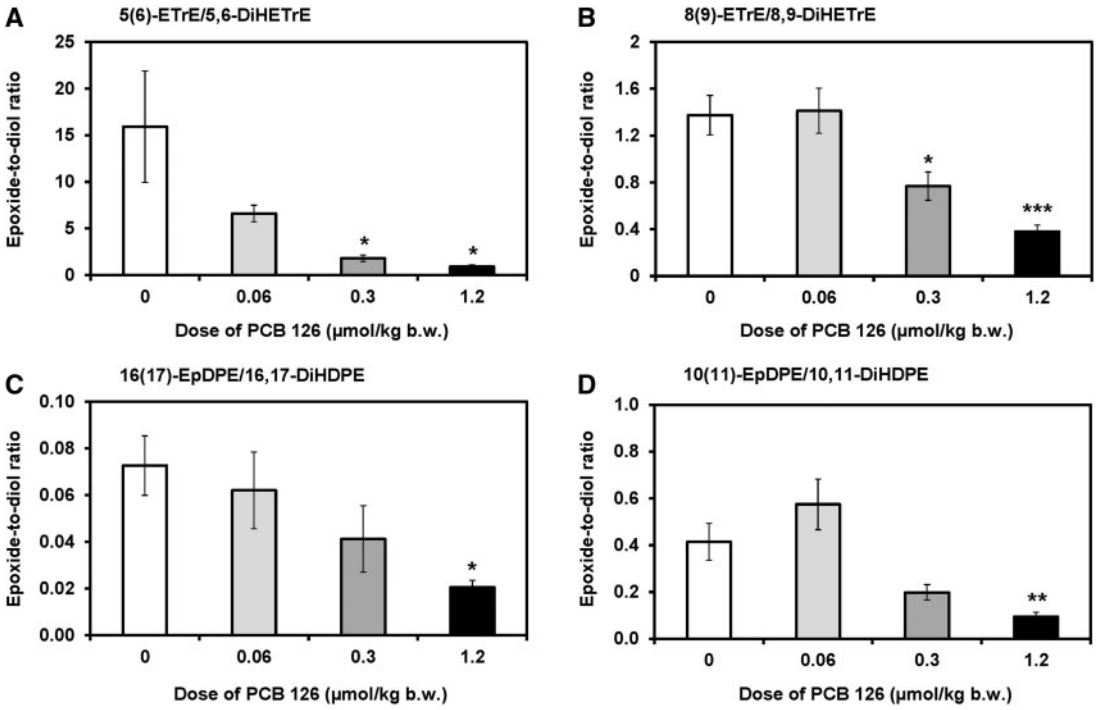

FIG. 7. The epoxide-to-diol metabolite ratios of several oxylipins decreased in a dose-dependent manner in the liver from PCB 126-treated male rats, as determined by metabolomics profiling with liquid chromatography-tandem mass spectrometry. Shown are representative examples of epoxide-to-diol ratios of oxylipins derived from **(A and B)** ARA and **(C and D)** DHA. See Supplementary Table S10 for a complete summary of epoxide-to-diol ratios. Data are presented as the mean ± SEM ($n = 10$ for control or $n = 8$ for PCB treatment groups). Dunnett's multiple testing correction procedure was used to compare PCB 126 treatment with the corn oil control. Significantly different from control $^{*}P < .05$; $^{**}P < .01$; $^{***}P < .001$.

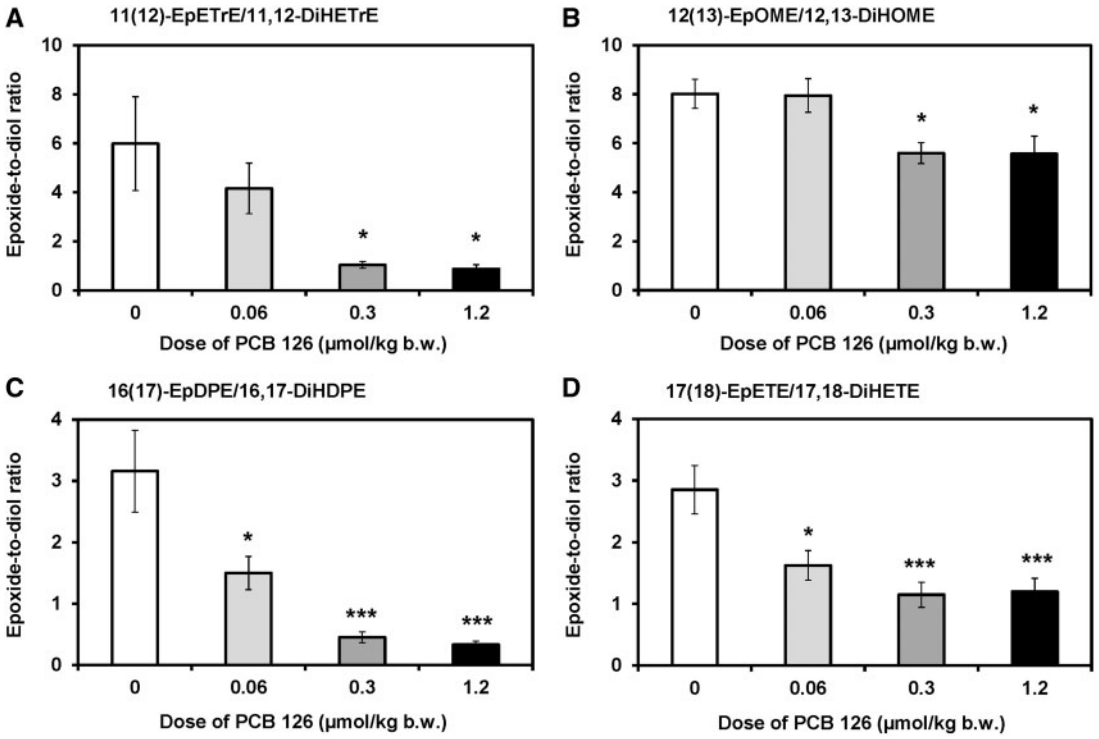

FIG. 8. The epoxide-to-diol metabolite ratios decreased in a dose-dependent manner in plasma from PCB 126-treated male rats for several oxylipins, as determined by metabolomics profiling with liquid chromatography-tandem mass spectrometry. Shown are representative examples of epoxide-to-diol ratios of oxylipins derived from **(A)** ARA, **(B)** LA, **(C)** DHA, and **(D)** EPA. See Supplementary Table S10 for a complete summary of epoxide-to-diol ratios. Data are presented as the mean ± SEM ($n = 10$ for control or $n = 8$ for PCB treatment groups). Dunnett's multiple testing correction procedure was used to compare PCB 126 treatment with the corn oil control. Significantly different from control $^{*}P < .05$; $^{***}P < .001$.

hydrolase hydrates PUFA epoxides (Fer *et al.*, 2008), microsomal epoxide hydrolase probably made only a minor contribution to the altered epoxide-to-diol levels in our study. Not only is sEH more abundant in the liver, but it also catalyzes the hydrolysis of PUFA epoxides more efficiently and has a different substrate selectivity than microsomal epoxide hydrolase (Morisseau and Hammock, 2013). Moreover, microsomal epoxide hydrolase activity was not altered in a clear, dose-dependent manner in the present study. PUFA epoxides may also be oxidized further by P450 enzymes or prostaglandin endoperoxide H synthases, undergo β-oxidation to shorter-chain fatty acids, form glutathione conjugates or are incorporated into phospholipids (Zeldin, 2001). Because dioxin-like PCB congeners are known to significantly increase glutathione transferase activity in the rat liver (Schramm *et al.*, 1985), it is possible that the glutathione transferase-catalyzed conversion of PUFA epoxides to glutathione conjugates also modulated hepatic and systemic PUFA epoxide levels in our study. Although limited experimental evidence demonstrates that PUFA epoxides are substrates of purified cytosolic glutathione transferases (Spearman *et al.*, 1985), it remains unknown to which extent this metabolic pathway is relevant *in vivo* and, thus, altered by PCB 126 treatment.

In this study, PCB 126 treatment resulted in a significant, dose-dependent increase in the levels of ARA, EPA and DHA-derived diols in the liver and, despite the increase in hepatic PUFA epoxide levels, altered the epoxide-to-diol ratio in favor of the diols. Similar effects of TCDD treatment on hepatic levels of PUFA diols have been reported in chick embryos and mice (Bui *et al.*, 2012; Diani-Moore *et al.*, 2014; Yang *et al.*, 2013). The increase in levels of PUFA diols is the result of several PCB 126-mediated effects *in vivo*. For example, acute TCCD treatment not only alters the lipid homeostasis in the liver, but also increases hepatic levels of PUFAs (Forgacs *et al.*, 2012) and induces the expression phospholipase A2 in rats (Bui *et al.*, 2012; Forgacs *et al.*, 2012) by mechanisms involving AhR (Leslie, 2015). Moreover, treatment with AhR agonists increases the expression and activity of sEH. For example, PCB 126 significantly increased the activity of cytosolic and peroxisomal sEH in this study. The AhR agonist benzo[a]pyrene similarly increased the hepatic expression of sEH in rats (Aboutabl *et al.*, 2011). It is currently unknown whether the increased cytosolic and peroxisomal sEH activity is mediated by AhR and/or a result of the altered lipid homeostasis following PCB 126 treatment. Overall, the increased expression and/or activity of enzymes involved in the formation oxylipins in the P450/sEH pathway is consistent with the shift of the epoxide-to-diol ratio towards a more inflammatory state of the liver following PCB 126 exposure.

The liver is a major source for PUFA epoxides and diols in the systemic circulation (Schuck *et al.*, 2014), and plasma levels of PUFA epoxides and diols to some extent reflected the activation of the P450/sEH pathway in the liver due to PCB 126 treatment in this study. Specifically, plasma levels of PUFA diols derived from ARA, EPA, and DHA showed a clear dose dependent increase in PCB 126-treated rats. In particular levels of 5,6-DiHETrE were a sensitive marker of PCB 126 exposure in rats and were significantly increased in all PCB 126 treatment groups compared with control. In contrast, plasma levels of the corresponding PUFA epoxides tended to decrease in PCB 126-treated rats, thus resulting in a decrease in plasma epoxide-to-diol ratios of several oxylipins. In particular ratios of 16(17)-EpDPE/16,17-DiHDPE and 17(18)-EpETE/17,18-DiHETE were significantly different from control at all PCB 126 doses investigated (Figure 8) and, consequently, are a sensitive marker of PCB 126 exposure. Similarly, TCDD treatment resulted in an AhR-mediated increase in serum, liver, and lung levels of 5,6-DiHETrE, an ARA-derived oxylipin, in male and female mice (Bui *et al.*, 2012; Yang *et al.*, 2013). Only a few studies have investigated a link between 5,6-DiHETrE levels and toxicant exposure. *In vitro* studies demonstrate that formation rates of 5,6-DiHETrE and other DiHETrE by mouse heart liver microsomes can be altered due to polycyclic aromatic hydrocarbon or mercury-mediated changes in the P450 enzyme system (Aboutabl *et al.*, 2009; Amara *et al.*, 2014). However, if these changes in *in vitro* ARA metabolism translate into changes of 5,6-DiHETrE levels in the systemic circulation, this has not been established. There is also evidence that the antimicrobial triclocarban, an environmental pollutant that inhibits sEH, decreases levels of oxylipins, including 5,6-DiHETrE, in mice (Liu *et al.*, 2011). Taken together, these observations suggest that 5,6-DiHETrE levels and/or ratios of 16(17)-EpDPE/16,17-DiHDPE and 17(18)-EpETE/17,18-DiHETE are potential biomarkers of exposure to PCB 126 and other AhR agonists. Because PUFA epoxides and diols are excreted by rodents and humans with the urine and can be readily quantified by LC/MS/MS (Newman *et al.*, 2002), oxylipins deserve further attention as potential biomarkers of exposure to AhR agonists, such as PCB 126, in laboratory and human studies.

Our findings demonstrate that the PCB 126-mediated activation of the P450/sEH pathway results in decreased epoxide-to-diol ratios, which is typically associated with pro-inflammatory disease phenotypes (Morisseau and Hammock, 2013). Indeed, several studies in rodents (Klaren *et al.*, 2016; Wang *et al.*, 2016) as well as a 2-year bioassay in female rats (NTP, 2006) demonstrate that PCB 126 exposure causes inflammation in the liver. At the same time, PCB 126 treatment had little-to-no effect on hepatic or circulating levels of several other regulatory oxylipins, such as 20-HETE. Interestingly, deactivation of the P450/sEH pathway in a mouse model of nonalcoholic fatty liver disease also resulted in a statistically significant decrease in PUFA epoxide levels, lower epoxide-to-diol ratios, and hepatic inflammation in mice on an atherogenic diet compared with controls on a standard rodent diet (Schuck *et al.*, 2014). Together, these observations demonstrate that dysfunction of the P450/sEH pathway due to environmental factors shifts hepatic and systemic epoxide-to-diol ratios towards a proinflammatory phenotype. Consequently, sEH may be a potential therapeutic target to attenuate toxicity caused by PCB 126 and other environmental factors in the liver. Indeed, there is evidence that genetic and pharmacological inhibition of sEH increases hepatic epoxide-to-diol ratios and attenuates hepatic inflammation in laboratory models (Diani-Moore *et al.*, 2014; Liu *et al.*, 2012; Schuck *et al.*, 2014). Alternatively, drugs under investigation for the treatment of nonalcoholic steatohepatitis, such as the phosphodiesterase inhibitor pentoxifylline (Zein *et al.*, 2012), may represent an approach to reduce hepatotoxicity associated with exposure to PCB 126 and other AhR agonists. Further studies are therefore needed to demonstrate that inhibition of sEH or other cellular targets in the P450/sEH pathway have similar effects in laboratory models of PCB 126 liver toxicity.

SUPPLEMENTARY DATA

Supplementary data are available online at http://toxsci.oxfordjournals.org/.

ACKNOWLEDGMENTS

The authors thank Kai Wang for advice regarding the statistical analysis; Austin Kammerer for help with the PCB

analysis; and Miao Li, Hua Shen, Kiran Dhakal, and Susanne Flor for help with the animal study.

FUNDING

This work was supported by the National Institute of Environmental Health Science at the National Institute of Health grant numbers (ES013661, ES04699, ES002710) and a K.C. Donnelly externship award to X.W. supporting a cooperative research study of the University of Iowa and UC Davis Superfund Research Centers.

REFERENCES

Aboutabl, M. E., Zordoky, B. N., and El-Kadi, A. O. (2009). 3-Methylcholanthrene and benzo(a)pyrene modulate cardiac cytochrome P450 gene expression and arachidonic acid metabolism in male Sprague Dawley rats. *Br. J. Pharmacol.* **158**, 1808–1919.

Aboutabl, M. E., Zordoky, B. N., Hammock, B. D., and El-Kadi, A. O. (2011). Inhibition of soluble epoxide hydrolase confers cardioprotection and prevents cardiac cytochrome P450 induction by benzo(a)pyrene. *J. Cardiovasc. Pharmacol.* **57**, 273–281.

Alvarez-Lloret, P., Lind, P. M., Nyberg, I., Orberg, J., and Rodríguez-Navarro, A. B. (2009). Effects of 3,3',4,4',5-pentachlorobiphenyl (PCB126) on vertebral bone mineralization and on thyroxin and vitamin D levels in Sprague-Dawley rats. *Toxicol. Lett.* **187**, 63–68.

Amara, I. E., Elshenawy, O. H., Abdelrady, M., and El-Kadi, A. O. (2014). Acute mercury toxicity modulates cytochrome P450, soluble epoxide hydrolase and their associated arachidonic acid metabolites in C57Bl/6 mouse heart. *Toxicol. Lett.* **226**, 53–62.

Bandiera, S., Safe, S., and Okey, A. B. (1982). Binding of polychlorinated biphenyls classified as either phenobarbitone, 3-methylcholanthrene or mixed-type inducers to cytosolic Ah receptor. *Chem. Biol. Interact.* **39**, 259–277.

Bhathena, A., Lee, C., and Riddick, D. S. (2002). Suppression of cytochrome P450 2C11 by aromatic hydrocarbons: Mechanistic insights from studies of the 5'-flanking region of the CYP2C11 gene. *Drug Metab. Dispos.* **30**, 1385–1392.

Bui, P., Solaimani, P., Wu, X., and Hankinson, O. (2012). 2,3,7,8-Tetrachlorodibenzo-p-dioxin treatment alters eicosanoid levels in several organs of the mouse in an aryl hydrocarbon receptor-dependent fashion. *Toxicol. Appl. Pharmacol.* **259**, 143–151.

Chen, J. J., Chen, G. S., and Bunce, N. J. (2003). Inhibition of CYP 1A2–dependent MROD activity in rat liver microsomes: An explanation of the hepatic sequestration of a limited subset of halogenated aromatic hydrocarbons. *Environ. Toxicol.* **18**, 115–119.

Chu, I., Villeneuve, D. C., Yagminas, A., Lecavalier, P., Poon, R., Feeley, M., Kennedy, S. W., Seegal, R. F., Hakansson, H., Ahlborg, U. G., *et al.* (1994). Subchronic toxicity of 3,3',4,4',5-pentachlorobiphenyl in the rat. 1. Clinical, biochemical, hematological, and histopathological changes. *Fundam. Appl. Toxicol* **22**, 457–468.

Chu, S., Covaci, A., and Schepens, P. (2003). Levels and chiral signatures of persistent organochlorine pollutants in human tissues from Belgium. *Environ. Res.* **93**, 167–176.

Decastro, B. R., Korrick, S. A., Spengler, J. D., and Soto, A. M. (2006). Estrogenic activity of polychlorinated biphenyls present in human tissue and the environment. *Environ. Sci. Technol.* **40**, 2819–2825.

Dhakal, K., Uwimana, E., Adamcakova-Dodd, A., Thorne, P. S., Lehmler, H. J., and Robertson, L. W. (2014). Disposition of phenolic and sulfated metabolites after inhalation exposure to 4-chlorobiphenyl (PCB3) in female rats. *Chem. Res. Toxicol.* **27**, 1411–1420.

Diani-Moore, S., Ma, Y., Gross, S. S., and Rifkind, A. B. (2014). Increases in levels of epoxyeicosatrienoic and dihydroxyeicosatrienoic acids (EETs and DHETs) in liver and heart in vivo by 2,3,7,8-tetrachlorodibenzo-*p*-dioxin (TCDD) and in hepatic EET:DHET ratios by cotreatment with TCDD and the soluble epoxide hydrolase inhibitor AUDA. *Drug Metab. Dispos.* **42**, 294–300.

Diani-Moore, S., Papachristou, F., Labitzke, E., and Rifkind, A. B. (2006). Induction of CYP1A and CYP2-mediated arachidonic acid epoxygenation and suppression of 20-hydroxyeicosatetraenoic acid by imidazole derivatives including the aromatase inhibitor vorozole. *Drug Metab. Dispos.* **34**, 1376–1385.

Diliberto, J. J., Burgin, D. E., and Birnbaum, L. S. (1999). Effects of CYP1A2 on disposition of 2,3,7,8-tetrachlorodibenzo-*p*-dioxin, 2,3,4,7,8-pentachlorodibenzofuran, and 2,2',4,4',5,5'-hexachlorobiphenyl in CYP1A2 knockout and parental (C57BL/6N and 129/Sv) strains of mice. *Toxicol. Appl. Pharmacol.* **159**, 52–64.

Doull, J. (2003). The "Red Book" and other risk assessment milestones. *Hum. Ecol. Risk Assess.* **9**, 1229–1238.

El-Sherbeni, A. A., and El-Kadi, A. O. S. (2014). Characterization of arachidonic acid metabolism by rat cytochrome P450 enzymes: The involvement of CYP1As. *Drug Metab. Dispos.* **42**, 1498–1507.

Falck, J. R., Sun, L. M., Blair, I., Dishman, E., Martin, M. V., Waxman, D. J., Guengerich, F. P., and Capdevila, J. H. (1990). Cytochrome-P-450-dependent oxidation of arachidonic-acid to 16-, 17- and 18-hydroxyeicosatetraenoic acids. *J. Biol. Chem.* **265**, 10244–10249.

Fer, M., Dreano, Y., Lucas, D., Corcos, L., Salaun, J. P., Berthou, F., and Amet, Y. (2008). Metabolism of eicosapentaenoic and docosahexaenoic acids by recombinant human cytochromes P450. *Arch. Biochem. Biophys.* **471**, 116–125.

Fisher, J. W., Campbell, J., Muralidhara, S., Bruckner, J. V., Ferguson, D., Mumtaz, M., Harmon, B., Hedge, J. M., Crofton, K. M., Kim, H., *et al.* (2006). Effect of PCB 126 on hepatic metabolism of thyroxine and perturbations in the hypothalamic-pituitary-thyroid axis in the rat. *Toxicol. Sci.* **90**, 87–95.

Forgacs, A. L., Kent, M. N., Makley, M. K., Mets, B., DelRaso, N., Jahns, G. L., Burgoon, L. D., Zacharewski, T. R., and Reo, N. V. (2012). Comparative metabolomic and genomic analyses of TCDD-elicited metabolic disruption in mouse and rat liver. *Toxicol. Sci.* **125**, 41–55.

Harris, T. R., Bettaieb, A., Kodani, S., Dong, H., Myers, R., Chiamvimonvat, N., Haj, F. G., and Hammock, B. D. (2015). Inhibition of soluble epoxide hydrolase attenuates hepatic fibrosis and endoplasmic reticulum stress induced by carbon tetrachloride in mice. *Toxicol. Appl. Pharmacol.* **286**, 102–111.

Hornsten, L., Bylund, J., and Oliw, E. H. (1996). Dexamethasone induces bisallylic hydroxylation of polyunsaturated fatty acids by rat liver microsomes. *Arch. Biochem. Biophys.* **332**, 261–268.

Hu, D., and Hornbuckle, K. C. (2010). Inadvertent polychlorinated biphenyls in commercial paint pigments. *Environ. Sci. Technol.* **44**, 2822–2827.

Hu, X., Lehmler, H. J., Adamcakova-Dodd, A., and Thorne, P. S. (2013). Elimination of inhaled 3,3'-dichlorobiphenyl and the

formation of the 4-hydroxylated metabolite. *Environ. Sci. Technol.* **47**, 4743–4751.

Huang, S. W., and Gibson, G. G. (1991). Differential induction of cytochromes-P450 and cytochrome-P450-dependent arachidonic-acid metabolism by 3,4,5,3',4'-pentachlorobiphenyl in the rat and the guinea-pig. *Toxicol. Appl. Pharmacol.* **108**, 86–95.

Kania-Korwel, I., Shaikh, N., Hornbuckle, K. C., Robertson, L. W., and Lehmler, H. J. (2007). Enantioselective disposition of PCB 136 (2,2',3,3',6,6'-hexachlorobiphenyl) in C57BL/6 mice after oral and intraperitoneal administration. *Chirality* **19**, 56–66.

Kashimoto, T., Miyata, H., Takayama, K., and Ogaki, J. (1987). [Levels of PCDDs, coplanar PCBs and PCDFs in patients with yusho and the causal oil by HR-GC.HR-MS]. *Fukuoka Igaku Zasshi* **78**, 325–336.

Klaren, W. D., Flor, S., Gibson-Corley, K. N., Ludewig, G., and Robertson, L. W. (2016). Metallothionein's role in PCB126 induced hepatotoxicity and hepatic micronutrient disruption. *Toxicol. Rep.* **3**, 21–28.

Koga, N., Beppu, M., and Yoshimura, H. (1990). Metabolism in vivo of 3,4,5,3',4'-pentachlorobiphenyl and toxicological assessment of the metabolite in rats. *J. Pharmacobiodyn.* **13**, 497–506.

Konkel, A., and Schunck, W. H. (2011). Role of cytochrome P450 enzymes in the bioactivation of polyunsaturated fatty acids. *Biochim. Biophys. Acta* **1814**, 210–222.

Lai, I., Chai, Y., Simmons, D., Luthe, G., Coleman, M. C., Spitz, D., Haschek, W. M., Ludewig, G., and Robertson, L. W. (2010). Acute toxicity of 3,3',4,4',5-pentachlorobiphenyl (PCB 126) in male Sprague-Dawley rats: Effects on hepatic oxidative stress, glutathione and metals status. *Environ. Int.* **36**, 918–923.

Lai, I., Chai, Y., Simmons, D., Watson, W. H., Tan, R., Haschek, W. M., Wang, K., Wang, B., Ludewig, G., and Robertson, L. W. (2011). Dietary selenium as a modulator of PCB 126-induced hepatotoxicity in male Sprague-Dawley rats. *Toxicol. Sci.* **124**, 202–214.

Lai, I. K., Dhakal, K., Gadupudi, G. S., Li, M., Ludewig, G., Robertson, L. W., and Olivier, A. K. (2012). N-acetylcysteine (NAC) diminishes the severity of PCB 126-induced fatty liver in male rodents. *Toxicology* **302**, 25–33.

Lai, I. K., Klaren, W. D., Li, M., Wels, B., Simmons, D. L., Olivier, A. K., Haschek, W. M., Wang, K., Ludewig, G., and Robertson, L. W. (2013). Does dietary copper supplementation enhance or diminish PCB126 toxicity in the rodent liver? *Chem. Res. Toxicol.* **26**, 634–644.

Lambert, G. H., Needham, L. L., Turner, W., Lai, T. J., Patterson, D. G., and Guo, Y. L. (2006). Induced CYP1A2 activity as a phenotypic biomarker in humans highly exposed to certain PCBs/PCDFs. *Environ. Sci. Technol.* **40**, 6176–6180.

Lauby-Secretan, B., Loomis, D., Grosse, Y., El Ghissassi, F., Bouvard, V., Benbrahim-Tallaa, L., Guha, N., Baan, R., Mattock, H., and Straif, K. (2013). Carcinogenicity of polychlorinated biphenyls and polybrominated biphenyls. *Lancet Oncol.* **14**, 287–288.

Leslie, C. C. (2015). Cytosolic phospholipase A2: Physiological function and role in disease. *J. Lipid Res.* **56**, 1386–1402.

Li, N., Liu, J. Y., Qiu, H., Harris, T. R., Sirish, P., Hammock, B. D., and Chiamvimonvat, N. (2011). Use of metabolomic profiling in the study of arachidonic acid metabolism in cardiovascular disease. *Congest. Heart Fail.* **17**, 42–46.

Liu, J. Y., Qiu, H., Morisseau, C., Hwang, S. H., Tsai, H. J., Ulu, A., Chiamvimonvat, N., and Hammock, B. D. (2011). Inhibition of soluble epoxide hydrolase contributes to the anti-inflammatory effect of antimicrobial triclocarban in a murine model. *Toxicol. Appl. Pharmacol.* **255**, 200–206.

Liu, Y., Dang, H., Li, D., Pang, W., Hammock, B. D., and Zhu, Y. (2012). Inhibition of soluble epoxide hydrolase attenuates high-fat-diet-induced hepatic steatosis by reduced systemic inflammatory status in mice. *PLoS One* **7**, e39165.

Lowry, O. H., Rosenbrough, N. J., Rarr, A. L., and Randall, R. J. (1951). Protein measurement with Folin Phenol reagent. *J. Biol. Chem.* **193**, 265–275.

Morisseau, C., and Hammock, B. D. (2007). Measurements of soluble epoxide hydrolase (sEH) activity. In *Techniques for Analysis of Chemical Biotransformation. Current Protocols in Toxicology* (J.S. Bus, L.G. Costa, E. Hodgson, D.A. Lawrence and D.J. Reed, Eds.), pp. 4.1–4.18. John Wiley & Sons, New Jersey.

Morisseau, C., and Hammock, B. D. (2013). Impact of soluble epoxide hydrolase and epoxyeicosanoids on human health. *Annu. Rev. Pharmacol. Toxicol.* **53**, 37–58.

Nerurkar, P. V., Park, S. S., Thomas, P. E., Nims, R. W., and Lubet, R. A. (1993). Methoxyresorufin and benzyloxyresorufin: Substrates preferentially metabolized by cytochromes P4501A2 and 2B, respectively, in the rat and mouse. *Biochem. Pharmacol.* **46**, 933–943.

Newman, J. W., Morisseau, C., and Hammock, B. D. (2005). Epoxide hydrolases: Their roles and interactions with lipid metabolism. *Prog. Lipid Res.* **44**, 1–51.

Newman, J. W., Watanabe, T., and Hammock, B. D. (2002). The simultaneous quantification of cytochrome P450 dependent linoleate and arachidonate metabolites in urine by HPLC-MS/MS. *J. Lipid Res.* **43**, 1563–1578.

NTP. (2006). NTP toxicology and carcinogenesis studies of 3,3',4,4',5-pentachlorobiphenyl (PCB 126) (CAS No. 57465-28-8) in female Harlan Sprague-Dawley rats (Gavage Studies). *Natl. Toxicol. Program. Tech. Rep. Ser.* 4–246.

Parkinson, A., Cockerline, R., and Safe, S. (1980). Polychlorinated biphenyl isomers and congeners as inducers of both 3-methylcholantrene and phenobarbitone type microsomal activity. *Chem. Biol. Interact.* **29**, 277–289.

Parkinson, A., Safe, S. H., Robertson, L. W., Thomas, P. E., Ryan, D. E., Reik, L. M., and Levin, W. (1983). Immunochemical quantitation of cytochrome P-450 isozymes and epoxide hydrolase in liver microsomes from polychlorinated or polybrominated biphenyl-treated rats. A study of structure-activity relationships. *J. Biol. Chem.* **258**, 5967–5976.

Pearce, R. E., McIntyre, C. J., Madan, A., Sanzgiri, U., Draper, A. J., Bullock, P. L., Cook, D. C., Burton, L. A., Latham, J., Nevins, C., *et al.* (1996). Effects of freezing, thawing, and storing human liver microsomes on cytochrome P450 activity. *Arch. Biochem. Biophys* **331**, 145–169.

Pessah, I. N., Cherednichenko, G., and Lein, P. J. (2010). Minding the calcium store: Ryanodine receptor activation as a convergent mechanism of PCB toxicity. *Pharmacol. Ther.* **125**, 260–285.

Puri, P., Wiest, M. M., Cheung, O., Mirshahi, F., Sargeant, C., Min, H. K., Contos, M. J., Sterling, R. K., Fuchs, M., Zhou, H., *et al.* (2009). The plasma lipidomic signature of nonalcoholic steatohepatitis. *Hepatology* **50**, 1827–1838.

Rifkind, A. B. (2006). CYP1A in TCDD toxicity and in physiology - With particular reference to CYP dependent arachidonic acid metabolism and other endogenous substrates. *Drug Metab. Rev.* **38**, 291–335.

Rignall, B., Grote, K., Gavrilov, A., Weimer, M., Kopp-Schneider, A., Krause, E., Appel, K. E., Buchmann, A., Robertson, L. W., Lehmler, H. J., *et al.* (2013). Biological and tumor-promoting effects of dioxin-like and non-dioxin-like polychlorinated

biphenyls in mouse liver after single or combined treatment. *Toxicol. Sci* **133**, 29–41.

Schecter, A., Colacino, J., Haffner, D., Patel, K., Opel, M., Papke, O., and Birnbaum, L. (2010). Perfluorinated compounds, polychlorinated biphenyls, and organochlorine pesticide contamination in composite food samples from Dallas, Texas, USA. *Environ. Health Perspect.* **118**, 796–802.

Schramm, H., Robertson, L. W., and Oesch, F. (1985). Differential regulation of hepatic glutathione transferase and glutathione peroxidase activities in the rat. *Biochem. Pharmacol.* **34**, 3735–3739.

Schuck, R. N., Zha, W., Edin, M. L., Gruzdev, A., Vendrov, K. C., Miller, T. M., Xu, Z., Lih, F. B., DeGraff, L. M., Tomer, K. B., *et al.* (2014). The cytochrome P450 epoxygenase pathway regulates the hepatic inflammatory response in fatty liver disease. *PLoS One* **9**, e110162.

Shaban, Z., Soliman, M., El-Shazly, S., El-Bohi, K., Abdelazeez, A., Kehelo, K., Kim, H. S., Muzandu, K., Ishizuka, M., Kazusaka, A., and., *et al.* (2005). AhR and PPAR alpha: Antagonistic effects on CYP2B and CYP3A, and additive inhibitory effects on CYP2C11. *Xenobiotica* **35**, 51–68.

Spearman, M. E., Prough, R. A., Estabrook, R. W., Falck, J. R., Manna, S., Leibman, K. C., Murphy, R. C., and Capdevila, J. (1985). Novel glutathione conjugates formed from epoxyeicosatrienoic acids (EETs). *Arch. Biochem. Biophys.* **242**, 225–230.

USEPA. (2013), Polychlorinated Biphenyls (PCBs): Basic information. Available at: https://www.epa.gov/pcbs. Accessed May 17, 2016.

Van Birgelen, A. P. J. M., Van der Kolk, J., Fase, K. M., Bol, I., Poiger, H., Brouwer, A., and Van den Berg, M. (1994). Toxic potency of 3,3',4,4',5-pentachlorobiphenyl relative to and in combination with 2,3,7,8-tetrachlorodibenzo-*p*-dioxin in a subchronic feeding study in the rat. *Toxicol. Appl. Pharmacol.* **127**, 209–221.

Van den Berg, M., Birnbaum, L. S., Denison, M., De Vito, M., Farland, W., Feeley, M., Fiedler, H., Hakansson, H., Hanberg, A., Haws, L., *et al.* (2006). The 2005 World Health Organization reevaluation of human and mammalian toxic equivalency factors for dioxins and dioxin-like compounds. *Toxicol. Sci.* **93**, 223–241.

van Ede, K. I., Aylward, L. L., Andersson, P. L., van den Berg, M., and van Duursen, M. B. (2013). Tissue distribution of dioxin-like compounds: Potential impacts on systemic relative potency estimates. *Toxicol. Lett.* **220**, 294–302.

Vezina, C. M., Walker, N. J., and Olson, J. R. (2004). Subchronic exposure to TCDD, PeCDF, PCB126, and PCB153: Effect on hepatic gene expression. *Environ. Health Persp.* **112**, 1636–1644.

Wahlang, B., Song, M., Beier, J. I., Falkner, K. C., Al-Eryani, L., Clair, H. B., Prough, R. A., Osborne, T. S., Malarkey, D. E., States, J. C., and., *et al.* (2014). Evaluation of Aroclor 1260 exposure in a mouse model of diet-induced obesity and non-alcoholic fatty liver disease. *Toxicol. Appl. Pharmacol.* **279**, 380–390.

Wang, B., Klaren, W. D., Wels, B. R., Simmons, D. L., Olivier, A. K., Wang, K., Robertson, L. W., and Ludewig, G. (2016). Dietary manganese modulates PCB126 toxicity, metal status, and MnSOD in the rat. *Toxicol. Sci.* **150**, 15–26.

Watanabe, M. X., Kunisue, T., Ueda, N., Nose, M., Tanabe, S., and Iwata, H. (2013). Toxicokinetics of dioxins and other organochlorine compounds in Japanese people: Association with hepatic CYP1A2 expression levels. *Environ. Int.* **53**, 53–61.

Wu, X., Barnhart, C., Lein, P. J., and Lehmler, H. J. (2015). Hepatic metabolism affects the atropselective disposition of 2,2',3,3',6,6'-hexachlorobiphenyl (PCB 136) in mice. *Environ. Sci. Technol.* **49**, 616–625.

Wu, X., Pramanik, A., Duffel, M. W., Hrycay, E. G., Bandiera, S. M., Lehmler, H. J., and Kania-Korwel, I. (2011). 2,2',3,3',6,6'-Hexachlorobiphenyl (PCB 136) is enantioselectively metabolized to hydroxylated metabolites by rat liver microsomes. *Chem. Res. Toxicol.* **24**, 2249–2257.

Xu, L., Li, A. P., Kaminski, D. L., and Ruh, M. F. (2000). 2,3,7,8 Tetrachlorodibenzo-p-dioxin induction of cytochrome P4501A in cultured rat and human hepatocytes. *Chem. Biol. Interact.* **124**, 173–189.

Yang, J., Eiserich, J. P., Cross, C. E., Morrissey, B. M., and Hammock, B. D. (2012). Metabolomic profiling of regulatory lipid mediators in sputum from adult cystic fibrosis patients. *Free Radic. Biol. Med.* **53**, 160–171.

Yang, J., Schmelzer, K., Georgi, K., and Hammock, B. D. (2009). Quantitative profiling method for oxylipin metabolome by liquid chromatography electrospray ionization tandem mass spectrometry. *Anal. Chem.* **81**, 8085–8093.

Yang, J., Solaimani, P., Dong, H., Hammock, B., and Hankinson, O. (2013). Treatment of mice with 2,3,7,8-tetrachlorodibenzo-*p*-dioxin markedly increases the levels of a number of cytochrome P450 metabolites of omega-3 polyunsaturated fatty acids in the liver and lung. *J. Toxicol. Sci.* **38**, 833–836.

Zein, C. O., Lopez, R., Fu, X., Kirwan, J. P., Yerian, L. M., McCullough, A. J., Hazen, S. L., and Feldstein, A. E. (2012). Pentoxifylline decreases oxidized lipid products in nonalcoholic steatohepatitis: New evidence on the potential therapeutic mechanism. *Hepatology* **56**, 1291–1299.

Zeldin, D. C. (2001). Epoxygenase pathways of arachidonic acid metabolism. *J. Biol. Chem.* **276**, 36059–36062.